

SYNCHROTRON AGING IN FILAMENTED MAGNETIC FIELDS

J. A. EILEK,^{1,2} D. B. MELROSE,² AND M. A. WALKER²

Received 1996 February 28; accepted 1997 January 24

ABSTRACT

Magnetic fields in synchrotron sources are almost certainly inhomogeneous, mixing high-field and low-field regions. This inhomogeneity affects the evolution of a relativistic electron distribution function due to the rate of energy loss of the electrons changing as they move between the two regions. We present two models for the evolution of the distribution function, and discuss the results of these models in terms of the critical energies, or synchrotron frequencies, where the particle and photon spectra steepen. We find these critical frequencies are higher than would be the case if the electrons were confined to a homogeneous high-field region. We apply our results to the interpretation of extragalactic radio sources whose dynamical ages are known to be significantly greater than the ages inferred from their high-frequency spectral breaks.

Subject headings: ISM: magnetic fields — radiation mechanisms: nonthermal

1. INTRODUCTION

Magnetic fields in diffuse synchrotron sources are unlikely to be homogeneous and uniform throughout the source. In particular, high-quality images of extragalactic radio sources show that filamentary substructure is the rule rather than the exception. This appears in the jets when resolved (e.g., M87, Owen, Hardee, & Cornwell 1989; Cyg A, Perley, Dreher, & Cowan 1984), as well as in the lobes and tails (Cyg A; Fornax A, Fomalont et al. 1989; M87, Hines, Owen, & Eilek 1989; 3C 443, Comins & Owen 1991; or the wide-angle tailed sources, O’Donoghue, Owen, & Eilek 1990). In addition, studies of magnetized, turbulent plasmas in the Sun (e.g., Zwaan 1987) and in numerical simulations (e.g., Pouquet, Frisch, & Leorat 1976) find that the fields in these plasmas are intermittent: they occupy high-field filaments or flux ropes, separated by regions of much lower field-strength.

In addition, it is becoming increasingly clear that radio galaxies suffer from an “aging problem:” their dynamical ages are much larger, typically by a factor ~ 10 , than the age inferred from the frequency at which their radio spectrum steepens. This is a well-known problem for type I sources, where the relevant dynamical age is the flow time down the tail, ~ 100 Myr typically, but the simple synchrotron age is $\lesssim 10$ Myr (Owen et al. 1985; O’Donoghue, Eilek, & Owen 1993; Eilek 1997). It may also be a problem for type II sources. The spectral gradients in the lobes have been interpreted in terms of hot spot advance speed (Alexander & Leahy 1987; Carilli et al. 1991). However, given the short synchrotron ages in these sources, the lack of apparently old (steep-spectrum) sources remains a nagging problem (e.g., Baldwin 1982; Eilek 1993). We note that the split of type I and type II sources in parent galaxy luminosity as well as radio power (Owen 1993) argues against old type II sources evolving into type I’s. Furthermore, dynamical arguments which rely on lobe expansion and hot spot advance speeds seem to suggest that dynamical ages are several times longer than synchrotron ages (Eilek 1996). Finally, there is evidence that the radio spectrum in the well-studied Cyg A is not that predicted by simple aging theory (Katz-Stone, Rudnick, & Andersen 1993). A third example is the fact that in some jets the minimum possible travel time to the end of the jet is much longer than the synchrotron lifetime for the required high-energy particles. This is especially true of jets such as M87, which radiate in the optical as well as in the radio (e.g., Felten 1968; Meisenheimer, Röser, & Schlötelburg 1996), but it also holds for giant sources such as 3C 326 (Willis & Strom 1978).

In this paper we study the impact of inhomogeneous fields on the aging problem. The idea is simple: if a relativistic electron spends much of its life in a low-field region, and then moves into a high-field region in which it can radiate efficiently, on average it loses energy more slowly than if it were continuously in the high-field region. Thus the source “looks younger than it is” (e.g., Hughes 1979; O’Donoghue et al. 1993). Spangler (1979) noted a variant in which the low losses are attributed to the electrons having small pitch angles, rather than being in a weak field, with scattering to larger pitch angle having the analogous effect to propagation into a high-field region (see Melrose 1970). Our contribution is to quantify this effect by determining the evolution of the particle distribution function, and the consequent synchrotron spectrum, from an inhomogeneous source.

Current aging analyses rely on established synchrotron theory, which assumes that the particles are well mixed in a uniform magnetic field (e.g., Kardashev 1962; Pacholczyk 1970). We recapitulate the important features of what we call the standard theory, to define notation and to establish comparison points for our analysis. A single relativistic particle of momentum p in a magnetic field B loses energy at a rate

$$\frac{dp}{dt} = -b_0 B^2 p^2, \quad (1.1)$$

¹ Physics Department and Astrophysics Research Center, New Mexico Tech, Socorro, NM 87801.

² Research Centre for Theoretical Astrophysics, School of Physics, University of Sydney, NSW 2006, Australia.

with $b_0 = 4e^4/9m_e^4 c^6 = 4.9 \times 10^7$ cgs. Suppose that a distribution of electrons extending to arbitrarily large p is injected into the magnetic field at $t = 0$. Then equation (1.1) implies that, at time t , there are no particles above $p = p_{cs}(t)$, with

$$P_{cs}(t) = \frac{1}{b_0 B^2 t}. \quad (1.2)$$

Thus there must be a break in the distribution function (DF) at $p \leq p_{cs}(t)$ at time t . A particle at momentum p radiates most of its energy at a characteristic synchrotron frequency

$$\nu_{sy}(p, B) = \frac{3eB}{4\pi m_e^3 c^3} p^2. \quad (1.3)$$

The frequency spectrum from a single particle cuts off exponentially at higher ν . Thus the standard model, with an initial injection of electrons, implies a spectral cutoff above

$$\nu_{cs}(t) = \frac{1}{A^2 t^2}, \quad (1.4)$$

with $A^2 = 64\pi e^7 B^2 / 243 m_e^5 c^9$. We illustrate this standard spectrum and its aging in Figure 1.

For a continuous injection of a power-law spectrum $f(p) \propto p^{-b}$ starting at $t = 0$, the standard model implies, at time t , a break at about $p_{cs}(t)$ to $f(p) \propto p^{-(b+1)}$, that is, an increase in the particle spectral index by unity. A power-law DF $f(p) \propto p^{-b}$ produces a power-law synchrotron spectrum with emissivity $j_{sy}(\nu) \propto \nu^{-\alpha}$, where $\alpha = (b - 3)/2$. Hence an increase in b by unity at $p_{cs}(t)$ corresponds to an increase in α by 0.5 at $\nu_{cs}(t)$. Similarly, an initial electron power law, suffering from synchrotron losses without ongoing injection, steepens exponentially at ν_{cs} (assuming pitch-angle scattering is effective; e.g., Melrose 1970).

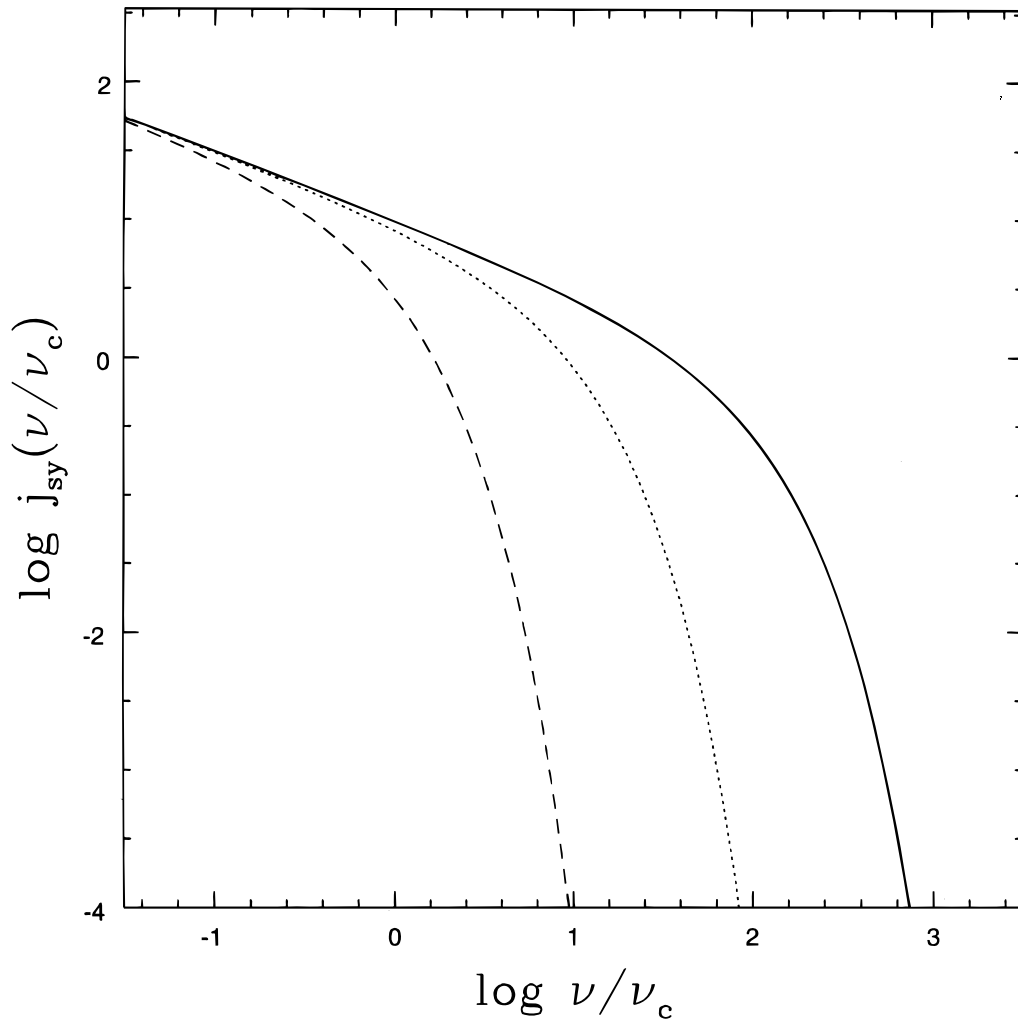


FIG. 1.—Synchrotron spectrum produced by a power-law distribution of electron energies radiating in a uniform magnetic field. The spectrum steepens at ν_c ; an approximate analytic form is $j(\nu) \propto \nu^{-\alpha} e^{-\nu/\nu_c}$, where α is the spectral index (Eilek & Arendt 1996). In the standard model, the critical frequency decays with time, as $\nu_c(t) \propto 1/t^2$. If we take the solid line as being the spectrum at $t = 1$, then the dotted line is at $t = 10^{1/2}$ and the dashed line at $t = 10$. Our solutions in the paper also find similar (but not identical) spectral shapes; however, the critical frequencies have a different dependence on time, as summarized in Table 1.

TABLE 1
CRITICAL FREQUENCIES FOR SPECTRAL TURNOVER

Model	Critical Frequency
Standard	$\nu_{eS}(t) = CB^{-3}t^{-2}$
Diffusion	$\nu_{e1}(t) = CB_H^{-3}t^{-2}(\tau/t)^{3/4}$
	$\nu_{e2}(t) = CB_H^{-3}t^{-2}(\tau/t)^{6/5}$
Leaky box	$\nu_{e0} = C\tau^{-2}B_H B_L^{-4}$

NOTE.—The constant $C = 243m_e^3 c^9 / 64\pi e^7$.

Observation of spectral bends allows one to use the standard model to infer an age for the source. It is the comparison of such estimated ages with other estimates (such as dynamical) of the age of a source that leads to the “aging problem.”

This standard analysis does not incorporate the effects of a nonuniform magnetic field. In this paper we consider a plasma which contains high-field regions separated by regions of low or zero field. We refer to the high-field regions as filaments, although a ropelike geometry is not essential to our models. The finite thickness, L , of the interfaces between the high- and low-field regions is important in one aspect of our discussion. We assume the particles are initially or continually injected into the low-field region, and slowly propagate into the high-field region. The propagation across field lines is probably diffusive in nature. Our solutions assume a diffusion coefficient D , and a “diffusion time” over scale L , $\tau = L^2/4D$. We return to the physical nature of the diffusion in § 4.

In this paper we present two different, but related, mathematical models which address the evolution of the DF and the synchrotron spectrum in a filamented magnetic field. For simplicity we assume that the source may be separated into two regions that are distinguished by the strength of the magnetic field: a high-field region and a low-field region. The high-field region is identified with the filaments, which may or may not be resolvable. The important assumption is that a given relativistic particle spends only a fraction of its time in the high-field region but its synchrotron losses are important only while it is in the high-field region.

In § 2 we present a detailed diffusion model. This model follows the detailed evolution of the electron distribution in physical space and in momentum space, while the electrons diffuse into the high-field region and simultaneously suffer synchrotron losses. This model allows us to find the spatial structure of the DF in the diffusion region, and of the consequent synchrotron spectrum. Because the diffusion region may well be unresolved in many observations, we also integrate spatially to find the composite synchrotron spectrum from the whole system. This model treats the low-field region as a very large reservoir of particles, and therefore does not allow any crossing of particles back from the high-field region to the low-field region. We therefore find the early development of this model, while the particles are actively diffusing, more interesting than its long-term asymptote, in which the particles are fully mixed with the high-field region.

In § 3 we present a “leaky box” model, similar to models of Galactic cosmic rays. The leaky box model is relevant to any situation, such as that envisaged here, where the particles diffuse back and forth between two different regions. The details of the diffusion are unimportant for many purposes, and the important parameters are the typical times spent by a particle in each region. This allows a major simplification, in that one can ignore spatial dependences and describe the effect on a typical particle through two parameters: the escape times from the first region into the second, and those from the second region into the first. This model then allows one to treat the long-term effects on a particle distribution of evolution in both regions. The application of this model to the steepening of the synchrotron spectra, as discussed in § 3, does not appear to have been considered previously.

Both our calculations find synchrotron spectra that steepen at high frequencies. However, both calculations find spectral breaks that are different, and generally higher at a given age, than the break predicted by the standard model (eq. [1.4]). We compare the break frequencies for the standard model and our two models, in Table 1. In § 4 we discuss the general trends of our two models and their quantitative application to the aging problem in radio sources.

2. A DIFFUSION MODEL

Our first approach is a formal diffusive solution, which incorporates the effects of simultaneous synchrotron losses. We picture two regions: a low-field region, which acts as a reservoir of particles, and a high-field region, into which the particles diffuse. The magnetic field increases along the z -axis from $\simeq 0$ in the low-field region to a maximum value B_H in the high-field region. We describe the variation in the form $B^2(z) = \zeta(z)B_H^2$, with $\zeta \rightarrow 0$ for $z \rightarrow 0$, and $\zeta \rightarrow 1$ as $z \rightarrow L$, where L is the characteristic width of the interface. The basic equation is

$$\frac{\partial f}{\partial t} = \frac{b_0 B_H^2 \zeta(z)}{p^2} \frac{\partial}{\partial p} (p^4 f) + D \frac{\partial^2 f}{\partial z^2}, \quad (2.1)$$

where D is the spatial diffusion coefficient, which we assume independent of particle energy.

2.1. Spatially Resolved Filaments

We solve equation (2.1) by a Fourier sine transform in space, and by the method of characteristics in momentum and time. One can find analytic solutions of equation (2.1) for the case when the reservoir contains a power-law distribution, $f_{\text{res}}(p) = \phi_0 p^{-b}$, with b an integer. Here we present solutions for $b = 4$, which show the important trends with the least algebraic complexity. Details are given in Appendix A.

The solution for the DF again has low- and high-energy behavior. For low energies we find

$$f(z, p, t) = \frac{\phi_0}{p^4} \operatorname{erfc} \left[\left(\frac{z^2}{4Dt} \right)^{1/2} \right], \quad b_0 B_H^2 \zeta(z) p t < 1, \quad (2.2)$$

and for high energies we find

$$f(z, p, t) = \frac{\phi_0}{p^4} \operatorname{erfc} \left[\left(\frac{b_0 B_H^2 p z^2}{4D} \right)^{1/2} \right], \quad b_0 B_H^2 \zeta(z) p t > 1. \quad (2.3)$$

The complementary error function has the limiting forms

$$\operatorname{erfc}(x) \simeq \begin{cases} 1 - \frac{2}{\sqrt{\pi}} x, & x \ll 1, \\ \frac{1}{\sqrt{\pi}} \frac{e^{-x^2}}{x} & x \gg 1. \end{cases} \quad (2.4)$$

At low energies synchrotron losses are unimportant and equation (2.2) reflects an energy-in-dependent spatial diffusion. The energy at which synchrotron losses become important, and the DF changes to the form in equation (2.3), depends on time and is given by

$$p_{c1}(z, t) = \frac{1}{b_0 B_H^2 \zeta(z) t}. \quad (2.5)$$

Below p_{c1} , the DF at a given (z, t) has the “reservoir” form, p^{-4} . Above p_{c1} , the DF has a non-power-law form which extends to a momentum

$$p_{c2}(z) = \frac{4D}{z^2 b_0 B_H^2}. \quad (2.6)$$

Above p_{c2} , the DF cuts off exponentially.

This DF maps to a synchrotron spectrum which depends on position in the filament. Since the distribution is not a simple power law, we cannot use the standard form for the spectrum. Rather, we follow the more general treatment of Eilek & Arendt (1996), writing the emissivity as³

$$j_{sy}(v, z) = 2\pi g_0 [\alpha_1 v B(z)]^{1/2} p_v^2 f(p_v), \quad (2.7)$$

with $g_0 = \sqrt{3} e^3 / 4\pi m_e c^3$ [noting that this is defined for a DF $n(p)$, the number per unit momentum; while Eilek & Arendt 1996 use a DF $n(E)$, the number per unit energy] and $\alpha_1 = 4\pi m_e^3 c^5 / 3e = 1.6 \times 10^{-19}$ cgs (from eq. [1.3]), and where the particle energy that gives the dominant contribution to the frequency spectrum at a given v is

$$p_v = \left[\frac{\alpha_1 v}{c^2 B(z)} \right]^{1/2}. \quad (2.8)$$

Note that p_v is a function of position, z .

Equation (2.7) may be written

$$j_{sy}(v, y) = j_0 B_H^{3/2} [\zeta(z)]^{3/4} v^{-1/2} \operatorname{erfc}(az), \quad (2.9)$$

with $j_0 = 2\pi\phi_0 g_0 c^2 \alpha_1^{-1/2}$, and $a = (4Dt)^{-1/2}$ for $b_0 B_H^2 \zeta p_v t < 1$, and $a = (Av^{1/2}/4D)^{1/2}$ for $b_0 B_H^2 \zeta p_v t > 1$ (with A defined as given after eq. [1.4]). The spectrum in equation 2.9 has two critical frequencies at which the spectrum breaks. The lower critical frequency comes from the condition $b_0 B_H^2 \zeta p_v t = 1$ and is

$$v_{c1} = \frac{v_{cS}(t)}{[\zeta(z)]^{3/2}}. \quad (2.10)$$

The higher critical frequency comes from the condition $b_0 B_H^2 z^2 p_v = 4D$, and is

$$v_{c2} = v_{cS}(t) [\zeta(z)]^{1/2} \left(\frac{4Dt}{z^2} \right)^2, \quad (2.11)$$

³ This expression arises from the full integral for $j_{sy}(v)$, taken over all particle energies, for the case of a single magnetic field. It is valid as long as the integral is not dominated by its limits, E_{\min} and E_{\max} , and for frequencies with $E_{\min} < E_v < E_{\max}$.

where $v_{cs}(t)$ follows from equation (1.4). Note that the t -dependences in equation (2.11) cancel, and that v_{c2} is not a function of time. The spatially resolved spectrum has three ranges. For low frequencies $\nu < v_{c1}$, we have

$$j_{sy}(\nu, z, t) \simeq j_0 B_H^{3/2} [\zeta(z)]^{3/4} \nu^{-1/2} \left(1 - \frac{2}{\sqrt{\pi}} \frac{z}{\sqrt{4Dt}} \right), \quad (2.12)$$

where we assume $z \ll (4Dt)^{1/2}$ in expanding the complementary error function. For intermediate frequencies $v_{c1} < \nu < v_{c2}$, we have

$$j_{sy}(\nu, z, t) \simeq j_0 B_H^{3/2} [\zeta(z)]^{3/4} \nu^{-1/2} \left[1 - \left(\frac{\nu}{v_{c2}} \right)^{1/4} \right]. \quad (2.13)$$

For high frequencies, $\nu > v_{c2}$, the spectrum cuts off exponentially:

$$j_{sy}(\nu, z, t) \simeq \frac{j_0}{\sqrt{\pi}} B_H^{3/2} [\zeta(z)]^{3/4} \nu^{-1/2} \left(\frac{\nu}{v_{c2}} \right)^{-1/4} \exp \left[- \left(\frac{\nu}{v_{c2}} \right)^{1/4} \right]. \quad (2.14)$$

2.2. Unresolved Filaments

The foregoing results are directly relevant to spatially resolved filaments, where the spectral break is a function of position. It is useful to integrate over the filament volume in the case of unresolved filaments, giving a result that can be compared to the leaky box model in § 3.

We integrate over space to define

$$N(p, t) = 4\pi p^2 \int_0^\infty f(z, p, t) dz = \frac{\phi_0}{p^2} \int_0^\infty \text{erfc}(az) dz, \quad (2.15)$$

where a is as defined below equation (2.9). Referring to equations (2.2) and (2.3), we see that the form of $f(z, p, t)$ depends on position: equation (2.2) applies close to the boundary, and equation (2.3) farther into the filament.

When equation (2.15) is evaluated, we find three energy ranges. Details of the integration are in Appendix A. The limit $L \ll (4Dt)^{1/2}$ corresponds to the interesting case of a system that is not yet well mixed. The two critical energies that separate the ranges are

$$p_{c1} = p_{cs}(t) \left(\frac{\tau}{t} \right)^{1/2}, \quad p_{c2} = p_{cs}(t) \frac{\tau}{t}, \quad (2.16)$$

where we recall the definition of the diffusion time, τ , from equation (1.7). At low energies $p < p_{c1}$, the integrated solution is

$$N(p, t) \simeq \frac{\phi_0}{p^2} \left(\frac{4Dt}{\pi} \right)^{1/2}, \quad (2.17)$$

which corresponds to the reservoir power law $4\pi p^2 f(p) \propto p^{-2}$. At high energies, $p > p_{c2}$, the integrated DF steepens:

$$N(p, t) \simeq \frac{\phi_0}{p^{5/2}} \left(\frac{4D}{b_0 B_H^2} \right)^{1/2}. \quad (2.18)$$

Thus, the low-energy solution reflects the initial power law $N(p) \propto p^{-2}$, and grows proportionally to $t^{1/2}$. The high-energy solution is a slightly steeper, steady state power law, $N(p) \propto p^{-5/2}$. The DF in the intermediate energy range is not a power law but rather a smooth transition between the two; its explicit form is given in Appendix A.

We note that both critical energies, p_{c1} and p_{c2} , are higher than the cutoff that would apply in the fully mixed model, $p_{cs}(t)$, for times $t < \tau$. Thus, the DF appears “younger” than it should, until the particles have fully diffused through the region.

We can also find the net synchrotron emissivity, by integrating equation (2.9) through the source:

$$J_{sy}(\nu, t) = \int_0^\infty j_{sy}(z, \nu, t) dz = J_0 \nu^{-1/2} \int_0^\infty \zeta(z)^{3/4} \text{erfc}(az) dz, \quad (2.19)$$

with a as defined below equation (2.9) and with $J_0 = j_0 B_H^{3/2}$. There are two critical frequencies at which the spectrum changes shape. These are

$$\nu_{c1} = v_{cs}(t) \left(\frac{\tau}{t} \right)^{3/4}, \quad \nu_{c2} = v_{cs}(t) \left(\frac{\tau}{t} \right)^{6/5}, \quad (2.20)$$

and they are stored in Table 1. We note that these are not simply related to p_{c1} and p_{c2} , through the relation $v_{sy}(p) = p^2 B c^2 / \alpha_1$ (from eq. [1.3]), as one might expect. This is due to the inhomogeneity of the magnetic field, which affects the energy cutoff and the spectral mapping somewhat differently. In particular, we have

$$\nu_{c1} = v_{sy}(p_{c1}) \left(\frac{\tau}{t} \right)^{-1/4}; \quad \nu_{c2} = v_{sy}(p_{c2}) \left(\frac{\tau}{t} \right)^{-4/5}. \quad (2.21)$$

These spectral breaks are higher than a homogeneous standard case would predict. Thus again, for times less than τ , the integrated source appears younger than it should.

In this model we identify three frequency ranges. For low frequencies, $\nu < \nu_{c1}$,

$$J_{\text{sy}}(\nu, t) \simeq J_0 \frac{Dt}{L} \nu^{-1/2}, \quad (2.22)$$

and for high frequencies, $\nu > \nu_{c2}$,

$$J_{\text{sy}}(\nu, t) \simeq \frac{J_0 D}{A L} \nu^{-1}. \quad (2.23)$$

At intermediate frequencies, $\nu_{c1} < \nu < \nu_{c2}$, the synchrotron spectrum is not strictly a power law but rather a smooth curve joining these two regions. For young sources, $t < \tau$, this intermediate frequency range can be quite large; the spectrum would appear to be smoothly curved (in log-log space), rather than a simple combination of two power laws over a broad frequency range.

In this section we have modeled the particle distribution and synchrotron spectrum of particles diffusing up a magnetic ramp into a high-field region. We find that the spectrum has power-law asymptotes at low and high frequencies, but also has a mid-frequency form that is not simply a power law. In both the resolved case, equations (2.10) and (2.11), and the unresolved case, equations (2.20) and (2.21), the spectral breaks are higher than the standard case would predict, for times less than the diffusion time τ . Thus, we find again that such a source would appear younger than it truly is.

3. A LEAKY BOX MODEL

Our second approach is a leaky box model, in which relativistic electrons leak from one region into another and back again. This is adapted from the leaky box model for the escape of Galactic cosmic rays from the Galactic disk into the halo (e.g., Kardashev 1962; Ginzburg & Syrovatskii 1964, p. 283; Berezhinskii et al. 1990, p. 50). We envisage our two regions as having a low field, B_L , and a high field, B_H . The leaking allows particles to cross from one region to the other at fixed, energy-independent rates. This simulates an energy-independent diffusion rate for particles. (It is possible to adapt the model to allow for energy-dependent diffusion, but we do not do so here.) In region 1, particles are lost at a rate r_{11} , and these particles appear in region 2, described by a source term involving a rate r_{12} . Similarly, particles in region 2 are lost at a rate r_{22} , and these particles appear in region 1, described by a source term involving a rate r_{21} . In principle, we allow injection in both regions [source terms $Q_1(p)$, $Q_2(p)$]; but for most purposes we specialize to injection only in the weak- B region [$Q_2(p) = 0$], so that particles appear in the high- B region only by leaking from the weak- B region.

This model is described by the pair of equations

$$\frac{\partial f_1(p)}{\partial t} = \frac{1}{p^2} \frac{\partial}{\partial p} [b_0 B^2 p^4 f_1(p)] - r_{11} f_1(p) + r_{12} f_2(p) + Q_1(p), \quad (3.1)$$

and

$$\frac{\partial f_2(p)}{\partial t} = \frac{1}{p^2} \frac{\partial}{\partial p} [b_0 B^2 p^4 f_2(p)] - r_{22} f_2(p) + r_{21} f_1(p) + Q_2(p), \quad (3.2)$$

where all the r_{ij} rates are constant and energy-independent. Conservation of the total number of particles implies

$$r_{12} V_1 = r_{22} V_2, \quad r_{21} V_2 = r_{11} V_1, \quad (3.3)$$

where V_1 and V_2 are the volumes of regions 1 and 2, respectively. Equation (3.3) implies $r_{11} r_{22} = r_{12} r_{21}$. In § 4, below we discuss physical origins of these r 's; in this section they are assumed to be given constants.

3.1. Time-dependent Evolution

First, we seek a time-dependent solution in which there is injection only in region 1 [$Q_2(p) = 0$]. We have been unable to find a full analytic solution. However, an iterative approach allows one to develop an approximate solution in a systematic manner. The procedure is as follows: (1) Solve equation (3.1) for f_1 as a function of t ignoring the leakage from region 2, that is, omitting the term $r_{12} f_2$. (2) Solve equation (3.2) for f_2 with the leakage from region 1, that is, the term $r_{21} f_1$, as the source term. (3) Take leakage from region 2 into region 1 into account by adding the source term $r_{12} f_2$ in equation (3.1) as a perturbation, return to step 1, and repeat the procedure.

Step 1 gives

$$f_1(p, t) = \frac{1}{b_0 B_L^2 p^4} \int_p^{p_1} dp' p'^2 Q_1(p') \exp \left[\frac{r_{22}}{b_0 B_H^2} \left(\frac{1}{p'} - \frac{1}{p} \right) \right], \quad (3.4)$$

with $p_1 = p/(1 - b_0 B_L^2 p t)$. After inserting equation (3.4) in equation 3.2 with $Q_2(p) = 0$ and $f_2(p, t = 0) = 0$, step 2 gives

$$f_2(p, t) = \frac{1}{b_0 B_L^2 p^4} \int_p^{p_1} dp' p'^2 f_1(p', t') \exp \left[\frac{r_{22}}{b_0 B_H^2} \left(\frac{1}{p'} - \frac{1}{p} \right) \right], \quad (3.5)$$

with

$$t'(p, p', t) = t - \frac{1}{b_0 B_H^2} \left(\frac{1}{p} - \frac{1}{p'} \right).$$

The next step in the iteration is straightforward, but is of no particular interest here.

The integrals in equations (3.4) and (3.5) can be evaluated explicitly for an initial power-law injection, $Q_1(p) = Q_{10} p^{-b}$. For $b \neq 3$, equation (3.4) gives

$$f_1(p, t) = \frac{Q_0}{b_0 B_L^2(b-3)} p^{-(b+1)} \begin{cases} [1 - (1 - b_0 B_L^2 pt)^{b-3}] & \text{for } b_0 B_L^2 pt < 1, \\ 1 & \text{for } b_0 B_L^2 pt > 1. \end{cases} \quad (3.6)$$

At low $p \ll 1/b_0 B_L^2 t$, equation (3.6) implies that $f_1(p, t) = Q_{10} t p^{-b}$ increases linearly with t , with the same spectral index as the injection spectrum. At higher $p > 1/b_0 B_L^2 t$ the spectral index increases to $b + 1$.

Using equation (3.6) as the source term in equation (3.5) gives, for $B_H > B_L$,

$$f_2(p, t) = \frac{r_{21} Q_{10} p^{-(b+2)}}{b_0^2 B_H^2} \begin{cases} \left\{ \begin{aligned} & \frac{1}{B_L^2} \left[\frac{(1 - b_0 B_L^2 pt)^{2-b} - 1}{b-2} - \frac{(1 - b_0 B_L^2 pt)^{4-b} - 1}{b-3} \right] \\ & + \frac{1}{B_H^2} \left[\frac{(1 - b_0 B_L^2 pt)^{2-b} - (1 - b_0 B_H^2 pt)^{2-b}}{b-2} \right. \\ & \quad \left. - \frac{(1 - b_0 B_L^2 pt)^{4-b} - (1 - b_0 B_H^2 pt)^{4-b}}{b-3} \right] \end{aligned} \right\} & \text{for } p < \frac{1}{b_0 B_H^2 t}, \\ \left\{ \begin{aligned} & \frac{1}{B_L^2} \left[\frac{(1 - b_0 B_L^2 pt)^{2-b} - 1}{b-2} - \frac{(1 - b_0 B_L^2 pt)^{4-b} - 1}{b-3} \right] \\ & \times \frac{1}{B_L^2} \left[\frac{(1 - b_0 B_L^2 pt)^{2-b} - 1}{b-2} - \frac{(1 - b_0 B_L^2 pt)^{4-b} - 1}{b-3} \right] \\ & + \frac{1}{B_H^2} \left[\frac{(1 - b_0 B_L^2 pt)^{2-b}}{b-2} - \frac{(1 - b_0 B_L^2 pt)^{4-b}}{b-3} \right] \end{aligned} \right\} & \text{for } \frac{1}{b_0 B_H^2 t} < p < \frac{1}{b_0 B_L^2 t}, \\ \frac{1}{B_L^2} \left(-\frac{1}{b-2} + \frac{1}{b-3} \right) & \text{for } p > \frac{1}{b_0 B_L^2 t} \end{cases} \quad (3.7)$$

Thus, in region 2 there are two breaks, at $p_1 = 1/b_0 B_H^2 t$ and $p_2 = 1/b_0 B_L^2 t$. The distribution function steepens by unity at p_1 and steepens further by unity at p_2 .

At small $p < p_1$, the DF in equation (3.7) increases in proportion to t^2 and has a power law with index b . This may be understood as follows. At small p synchrotron losses are unimportant, so that the particle DF in region 1 builds up linearly with t . The DF in region 2 builds up due to leakage from region 1, so that it builds up proportional to t times the DF in region 1, giving the t^2 dependence. For $p_1 \lesssim p \lesssim p_2$, the DF (eq. [3.7]) increases in proportion to t and has a power law with index $b + 1$. This may be understood by considering the case $B_H^2 \gg B_L^2$ in which the synchrotron lifetime in region 2 is much shorter than that in region 1. Then the injection spectrum into region 2 due to leakage from region 1 is the low- p spectrum in region 1, which is proportional to t and has spectral index b . The synchrotron losses in region 2 cause this distribution to steepen at $p \gtrsim p_1$ to spectral index $b + 1$. For $p > p_2$, the distribution in equation (3.7) is a time-independent power law with index $b + 2$. This may be understood by noting that for large p synchrotron losses dominate. In region 1 the distribution results from injection balancing the losses, leading to a power law with spectral index $b + 1$. The distribution in region 1 acts as an injection spectrum into region 2, so that balancing injection and losses there steepen the spectral index further to $b + 2$.

The breaks in the resulting synchrotron spectrum are related to the breaks in the particle spectrum in the usual way, using equation (1.3). Thus the steepening in region 1, described by equation (3.6), implies a synchrotron spectrum whose spectral index increases by 0.5. Such a break is familiar as a standard signature of synchrotron aging. The synchrotron spectrum from region 2 has two breaks, both by 0.5, at the characteristic frequencies corresponding to particle momenta p_1 and p_2 in a magnetic field B_H :

$$v_{c1}(t) = \frac{c^2}{\alpha_1 b_0^2 B_H^3 t^2} = v_{cs}(t), \quad v_{c2}(t) = \frac{c^2 B_H}{\alpha_1 b_0^2 B_L^4 t^2} = v_{cs}(t) \frac{B_H}{B_L}. \quad (3.8)$$

3.2. Asymptotic, Steady State Solution

The time-dependent solution consisting of equations (3.6) and (3.7) applies only for early times. Once the distribution in region 2 builds up sufficiently, leakage back in region 1 modifies the distribution there. On a much longer timescale a balance between the two regions is approached. The resulting asymptotic solution may be found relatively easily.

The approach adopted here is to use a Laplace transform, which allows the possibility of a formal, analytic, time-dependent solution. The formal solution is derived in Appendix A, but we were unable to invert the Laplace transform explicitly. With s the conjugate variable to t , the asymptotic solution, $t \rightarrow \infty$, follows from the limit $s \rightarrow 0$ for the Laplace-transformed distribution functions. The asymptotic solution may be obtained for injection in either or both regions, but we consider only injection in the weaker field region 1.

The asymptotic solution in region 1 is

$$f_{1\infty} = \frac{1}{b_0 p^4} \int_p dp' p'^2 \left\{ \frac{Q_1(p)}{B_L^2} + C(\rho) \left[\frac{r_{11} Q_1(p)}{B_L^4} \right] \right\}, \quad (3.9)$$

and in region 2 is

$$f_{2\infty} = -\frac{1}{b_0 p^4} \int_p dp' p'^2 C(\rho) \left[\frac{r_{21} Q_1(p)}{B_L^4} \right], \quad (3.10)$$

with

$$\rho = p_0 \left(\frac{1}{p'} - \frac{1}{p} \right), \quad p_0 = \frac{1}{2b_0} \left(\frac{r_{11}}{B_L^2} + \frac{r_{22}}{B_H^2} \right) \quad (3.11)$$

and

$$C(\rho) = \frac{2e^\rho \sinh \rho}{r_{11} B_L^{-2} + r_{22} B_H^{-2}}. \quad (3.12)$$

The integrals in the solutions in equations (3.9) and (3.10) may be evaluated explicitly for our power law $Q_1(p)$. For region 1 the leading term in equation (3.9) gives $p^{-(b+1)}$ for $p \gg p_0$; that is, the usual injection-plus-losses power law. In region 2 the spectrum steepens at p_0 , being proportional to p^{-b} below p_0 and to $p^{-(b+2)}$ above p_0 . To understand this, note that the spectral index in region 1 increases by unity at p_0 , and this acts as a source spectrum for region 3. The spectrum proportional to $p^{-(b+1)}$ at $p > p_0$ injected into region 2 is modified by the synchrotron losses in region 2, causing the spectrum to bend by unity at $p = p_0$ and leading to a net bend by 2. These two bends occur at the same p_0 in this asymptotic case because the bends are determined by the mean synchrotron losses; specifically, an average of the momenta $r_{11}/b_0 B_L^2$ and $r_{22}/b_0 B_H^2$ at which bends occur over the relative mean times, $1/r_{11}$ and $1/r_{22}$, spent in the weak and strong regions, respectively.

We identify $r_{11} \simeq r_{22} \simeq 1/\tau$ as the inverse of the typical time τ to cross from one region to the other, and we take $B_H \gg B_L$. Then we have

$$p_0 \simeq \frac{1}{b_0 B_L^2 \tau} \simeq p_{cS}(t) \frac{B_H^2}{B_L^2} \frac{t}{\tau}, \quad (3.13)$$

which implies $p_0 \gg p_{cS}(t)$ for $t \gg \tau(B_L/B_H)^2$. Thus we expect the asymptotic solution to be approached for $t \gtrsim \tau(B_L/B_H)^2$. We note that it is the *low*-field value, $B_L \simeq 3 \mu\text{G}$, that determines p_0 , and not the high-field value, B_H , that would be used in the "standard" aging calculation.

The break in the DF implies a break in the frequency spectrum at

$$\nu_{c0} = \frac{c^2 B_H}{\alpha_1 b_0^2 B_L^4 \tau^2} = \nu_{cS}(t) \frac{B_H}{B_L} \frac{t^2}{\tau^2}. \quad (3.14)$$

This is stored in Table 1. We note two observational consequences. First, for $\nu_{c0} \gg \nu_{cS}(t)$, the interpretation of data in terms of normal synchrotron aging can be very misleading, leading to an underestimate of the age by a factor $\sim (B_L/B_H)^{3/2}$. Second, any variation of ν_{c0} with time must reflect secular changes in τ (the diffusion rate) or in the local magnetic fields B_L and B_H .

In this section we have modeled the particle distribution and synchrotron spectrum from a two-field system, in the limit where the particles move freely from one region to the other, at a rate $r_{11} \simeq r_{22} \simeq 1/\tau$. The combined synchrotron spectrum from the two regions depends on the ratios V_2/V_1 of the volumes and B_H/B_L of the magnetic fields. The most interesting case is $B_H \gg B_L$, with V_1/V_2 not too large, so that region 2 dominates in producing the net frequency spectrum. In this case, our time-dependent solutions (§ 3.1) should appear when the source is relatively young, $t < \tau(B_L/B_H)^2$. In principle both ν_{c1} and ν_{c2} are observable when region 2 dominates the total emission, but they are such widely separated frequencies that only one is likely to be seen in the observing range. In this case the source looks "normal," but if ν_{c2} is the cutoff seen, it can lead to a serious underestimate of the age of the source. For an older source, $t > \tau(B_L/B_H)^2$, we expect the asymptotic solution to apply, implying spectral bends given by equations (3.13) and (3.14). We then have $p_0 \gg p_{cS}$ and $\nu_{c0} \gg \nu_{cS}$, so that the source looks much younger than it truly is.

4. DISCUSSION: THE SOURCES CAN BE FOOLING US

In this paper we have presented two models for the evolution of an electron distribution due to synchrotron losses in an inhomogeneous field. Each model is somewhat idealized, but each allows us to find analytic solutions. The common feature of these models is that a given electron spends only a fraction of its time in the region where the field is strong, and it is this region that dominates in determining the synchrotron losses. Hence, each model results in an electron distribution that

produces a high-frequency turnover that is characteristic of the time spent in the high-field region, and not of the time since the electron was accelerated or injected into the system. Table 1 summarizes the solutions for the two models. These solutions allow one to quantify the apparent slowing down of the aging of the electron distribution.

4.1. Diffusion: Type I Sources?

In § 2 we modeled the particle distribution and synchrotron spectrum of electrons diffusing up a magnetic ramp into high-field region. This model addresses the details of diffusion in the interface between the high- and low-field regions. Diffusion through the magnetic ramp is tracked explicitly, with new particles being supplied by a semi-infinite reservoir at the edge. Physically, this reservoir may be a region with only initial particle acceleration, large enough not to be seriously depleted while particles diffuse into the high-field regions. Alternatively, the reservoir may be a region of ongoing in situ acceleration. We find time-dependent solutions for the DF, for times $t < \tau$ where $\tau = L^2/4D$ characterizes the time to diffuse into the high-field region. The energy and spectral breaks in these solutions are, of course, higher than would be the case if the particles were initially well mixed with the high-field region, simply because synchrotron energy losses are smaller in the low-field regions. In consequence, the synchrotron spectrum in this solution has a characteristic, broadly curved turnover region (from $\sim \nu_{c1}$ to $\sim \nu_{c2}$). Standard, two-frequency observations, interpreted in terms of the standard model, will erroneously identify a single turnover frequency, ν_c , and thus suggest a particle population which is “younger” than its real age. Multifrequency observations, however, should have the capability to distinguish between this solution and the more standard one.

Our diffusion model applies on times $t \ll \tau$, that is, for sources in which crossing back from region 2 to region 1 has not yet become important. It does not require ongoing acceleration in region 1 (although that is also possible). One application of this model may be to tailed, type I radio sources. As we pointed out in § 1, these sources suffer from severe aging problems: the dynamical time for flow down the tail is much longer than the homogeneous synchrotron age inferred from their radio spectra. The tail spectra do decay with distance down the tail, which would be consistent with the sense of spectral evolution found in § 2 (or Table 1). In order for this model to apply, the diffusion time τ must be longer than the flow time down the tail, which is typically ~ 100 Myr (e.g., O’Donoghue et al. 1993; Eilek 1997). We return to this point below.

4.2. The Leaky Box: Type II Sources?

In § 3 we modeled the particle distribution for a two-field system with particles diffusing back and forth between regions of high and low field. This model is large-scale, compared to the scale of the interface, and is parameterized by rates at which particles move from region 1 to region 2 and back again. Interesting solutions are those which maintain a high spectral break in region 2; these require ongoing injection in region 1 to offset the system-wide losses. When this is the case, then for times $t \gtrsim \tau B_L^2/B_H^2$, where τ characterizes the time to go between regions, the particle distribution tends to an asymptotic form, with a break at energy p_0 which does not change with time. This is because diffusion into region 2, supplied by ongoing injection in region 1, is fast enough to balance the rate at which particles at p_0 lose energy by synchrotron radiation. Thus, at long times, the source seems to have “stopped aging” in the sense that the spectral break remains constant: in a conventional analysis, it will appear younger than it is. This is demonstrated graphically in Figure 2, where we plot the evolution of the break frequency corresponding to the leaky box theory, and also the evolution of the corresponding homogeneous case ($\nu_c \propto t^{-2}$).

A possible application of this model is to type II radio sources. As we noted in § 1, despite the apparently sensible spectral aging rate inferred from spectral steepening in the lobes, the lack of steep-spectrum sources and possible discrepancies between dynamical and spectral ages also suggest an aging problem here. Application of our leaky box model requires an ongoing injection of fresh particles. The hot spots clearly provide this, and the particles stream easily through the low-field interfilament regions in the lobes. If we assume this is to be the case, our model predicts a standard exponential cutoff at ν_{c0} ; referring to equation (3.14) or Table 1 shows that ν_{c0} depends on the local magnetic field and diffusion rate, not on the age of

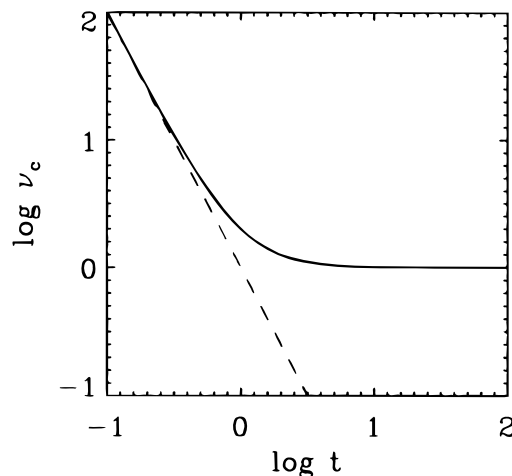


FIG. 2.—Characteristic evolution of the frequency, ν_c , at which the synchrotron spectrum changes slope (“breaks”) in the leaky box model (solid line). Time, t , is measured in units of the characteristic time $\tau B_L^2/B_H^2$, while the break frequency (ν_c) is measured in units of the asymptotic break frequency. The dashed line shows the evolution of the break frequency expected in the standard model.

the radiating plasma. Inserting numbers gives

$$\nu_{c0} \simeq \frac{2.4 \times 10^6}{\tau_{\text{Myr}}^2} \left(\frac{B_H}{B_L^4} \right)_{\mu\text{G}} \text{ GHz} . \quad (4.1)$$

Thus, picking for illustration $B_L \sim 10 \mu\text{G}$ and $B_H \sim 30 \mu\text{G}$, we find that $\tau \sim 85 \text{ Myr}$ is needed to give a 1 GHz turnover. Lower field values need higher τ 's, that is slower diffusion to fix ν_{c0} in the range required by observations.

4.3. Diffusion Rates

Both of our calculations rely on slow diffusion: a time constant $\sim 100 \text{ Myr}$ is called for if observed turnover frequencies and dynamical estimates of source ages are to be explained. Is this reasonable?

The diffusion is probably due to plasma turbulence. In the presence of MHD turbulence, the cross-field diffusion coefficient due to field-line wandering is

$$D \simeq \frac{c\lambda_t}{64\pi^2} \frac{\delta B^2}{B^2} . \quad (4.2)$$

where $\delta B^2/8\pi$ is the energy density of the Alfvén waves, and λ_t is its largest scale (Jokipii & Parker 1966). We write the turbulent spectrum in terms of its smallest wavenumber ($k_t = 2\pi/\lambda_t$), so that its energy density per wavenumber at k_t is $W(k_t) \simeq \lambda_t \delta B^2/16\pi^2$. We can estimate a mean free path, from the usual identification, $D = \frac{1}{3}\lambda_{\text{mfp}} c$, so

$$\frac{\lambda_{\text{mfp}}}{\lambda_t} \simeq \frac{3}{64\pi^2} \frac{\delta B^2}{B^2} , \quad (4.3)$$

and the effective mean free path is seen to be a small fraction of λ_t , as required for a diffusive treatment, even in the presence of strong turbulence (where one might have δB^2 as comparable to B^2). It seems most likely that $\lambda_t < L$: that the turbulent scale is less than the interface scale. The time particles take to diffuse a distance L is on the order of

$$\tau = \frac{L^2}{4D} \sim 0.5 \frac{B^2}{\delta B^2} L_{\text{kpc}} \frac{L}{\lambda_t} \text{ Myr} . \quad (4.4)$$

From observations of filamentary structure in radio lobes, we estimate the interface scale $L \lesssim 1 \text{ kpc}$. With this equation (4.4) shows that a diffusion time $\tau \sim 100 \text{ Myr}$ requires the turbulence satisfy

$$\frac{\delta B^2}{B^2} \frac{\lambda_t}{L} \sim 5 \times 10^{-3} . \quad (4.5)$$

Thus, turbulent diffusion can slow the mixing of electrons with field, if it is small scale or low amplitude. Without any direct measure of turbulent structures in these sources, we cannot corroborate this result (eq. [4.5]); we simply note that it must be satisfied if turbulent diffusion is to be relevant to the aging problem in these sources.

4.4. The Jet in M87

One source of particular interest with respect to particle aging is the jet of M87. Not only does the jet exhibit radio emission, but also optical/UV and even X-ray synchrotron emission is evident. Moreover, the optical/UV morphology bears a striking similarity to that seen in the radio. Conventional interpretation of the M87 jet has difficulty in explaining the morphological similarity across such a large range of frequencies because the high break frequency ($\nu_c \simeq 10^8 \text{ GHz}$) is conventionally taken to mean that the particle distribution is very young, and in turn this implies local particle acceleration. However, one expects that any local acceleration ought to produce a particle spectrum which reflects the local conditions, whereas the observed synchrotron spectrum is very similar throughout the jet, despite the highly structured and filamentary nature of the emission region. While this dichotomy does not exclude the possibility of in situ particle acceleration, it is certainly a problem for that viewpoint.

Owen et al. (1989) suggested—partly on the basis of the transverse limb-brightened morphology observed in the radio—that the M87 jet interior is largely free of magnetic field and serves as a low loss conduit for particles accelerated in the nucleus (see also Walker, Melrose, & Ball 1994). In this outlook it is easier to understand the global nature of the jet's synchrotron emission spectrum, as one starts with an essentially global electron spectrum; the electrons lose little of their energy as they propagate out in the postulated low-field interior of the jet. The theory we have developed is relevant to this case. There is, however, an extra complexity in that the geometry of the emission region takes the form of a hollow cone. In this geometry, particles that diffuse into the high-field (emission) region, from the jet interior, can subsequently diffuse further and be lost from the source completely. This is a possibility which is not accounted for in either of the treatments we have presented; qualitatively we can see that the effect acts to make the source appear younger still, as the particles that are lost from the source have, on average, spent more time in the high-field region than those nearer the inner boundary of the emission region. Using the physical parameters derived by Owen et al. (1989) ($B_H \sim 300 \mu\text{G}$, $L_{\text{kpc}} \lesssim 10^{-2}$) as input to the asymptotic theory of § 3.2, we estimate the break frequency as $\nu_c \gtrsim 10^{11} (\delta B^2/B^2)^2 \text{ GHz}$, so the observed break at 10^6 GHz is easily accounted for by relatively weak turbulence. Loss of electrons from the source, as they diffuse out of the jet, ought to raise this break frequency somewhat, for the reasons just given. However, the presence of the outer boundary means that we cannot make firm quantitative predictions concerning the M87 jet using this version of the theory, and we defer a proper discussion to a later paper.

We thank Dave Galloway for helpful suggestions. J. E. thanks the RCFTA for its support and hospitality during her visit there; her work was also partially supported by NSF grant AST 91-17029.

APPENDIX A

THE DIFFUSION MODEL

A1. THE SOLUTION METHOD

It is convenient to write $n(p, z, t) = 4\pi p^2 f(p, z, t)$, and then equation (2.1) becomes

$$\frac{\partial n}{\partial t} = b_0 B_H^2 \zeta(z) \frac{\partial}{\partial p} (p^2 n) + D \frac{\partial^2 n}{\partial z^2}. \tag{A1}$$

Our initial condition is $n(p, z, t = 0) = 0$ for $z > 0$, and we take $n(p, z = 0, t) = \phi_0 p^{-(b-2)}$. We define

$$q = b_0 B_H^2 p, \quad y = \frac{z}{\sqrt{D}}, \tag{A2}$$

and write equation (A1) as

$$\frac{dn}{ds} = \frac{\partial n}{\partial t} - q^2 \zeta(y) \frac{\partial n}{\partial q} = 2q \zeta(y) n + \frac{\partial^2 n}{\partial y^2}. \tag{A3}$$

The equations for the characteristics are

$$\frac{dt}{ds} = 1, \quad \frac{dq}{ds} = -\zeta(y) q^2. \tag{A4}$$

For $q\zeta t < 1$ (young particles) the appropriate solution of equation (A4) is

$$t = s, \quad \frac{1}{\zeta q} = s + \frac{1}{\tau}. \tag{A5}$$

We define the sine transform by

$$N(\lambda, s) = \sqrt{\frac{2}{\pi}} \int_0^\infty \sin(\lambda y) n(y, s) dy, \tag{A6}$$

and transform equation (A3) to find

$$\frac{dN}{ds} + \lambda^2 N(\lambda, t) - F(s, \tau) N = \lambda N_0(q), \tag{A7}$$

with $N_0(q) = (2/\pi)^{1/2} n(y = 0, q, t)$, and where $F(s, \tau)$ is the expression $2\zeta q$ written as a function of s and τ . The formal solution to equation (A7) is

$$N(s) e^{\beta(s)} = \int_0^s e^{\beta(s')} \lambda N_0 [q(s')] ds', \tag{A8}$$

where the function $\beta(s)$ is

$$\beta(s) = \int \left(\lambda^2 - \frac{2\tau}{1 + s\tau} \right) ds, \quad q\zeta t < 1. \tag{A9}$$

Solving for $N(\lambda, s)$ gives

$$N(\lambda, s) = \lambda \phi_0 e^{-\lambda^2 s} (1 + s\tau)^2 \int_0^s e^{\lambda^2 s'} (1 + s'\tau)^{-2} \left(\frac{\tau}{1 + s'\tau} \right)^{-(b-2)} ds', \tag{A10}$$

which integrates for $b = 4$ to

$$N(\lambda, s) = \frac{(1 + s\tau)^2 \phi_0}{\lambda \tau^2} (1 - e^{-\lambda^2 s}). \tag{A11}$$

Finally, carrying out the inverse sine transform, we get

$$n(y, q, t) = \frac{\phi_0}{p^2} \operatorname{erfc} \left(\frac{y}{2\sqrt{t}} \right) \tag{A12}$$

where $\text{erfc}(x)$ is the complementary error function.

For $q\zeta t > 1$ (old particles) the appropriate solution of equation (A4) is

$$t = \tilde{s} + \tilde{\tau}, \quad \frac{1}{\zeta q} = \tilde{s}. \quad (\text{A13})$$

In place of equations (A9), (A10), (A11), and (A12) we find, respectively,

$$\beta(s) = \int \left(\lambda^2 - \frac{2}{\tilde{s}} \right) ds, \quad q\zeta t > 1, \quad (\text{A14})$$

$$N(\lambda, \tilde{s}) = \lambda \phi_0 e^{\lambda^2 \tilde{s}} \int_0^{\tilde{s}} \tilde{s}'^b e^{\lambda^2 \tilde{s}'} d\tilde{s}', \quad (\text{A15})$$

$$N(\lambda, \tilde{s}) = \frac{\phi_0 \tilde{s}^2}{\lambda} (1 - e^{-\lambda^2 \tilde{s}}), \quad (\text{A16})$$

$$n(p, z, t) = \frac{\phi_0}{p^2} \text{erfc} \left(\frac{y\sqrt{q}}{2} \right). \quad (\text{A17})$$

A2. INTEGRATION OVER THE FILAMENT

On integrating either equation (A12) or equation (A17) over z , we write

$$N(p, t) = \int_0^\infty n(z, p, t) dz = \frac{\phi_0}{p^2} \int_0^\infty \text{erfc}(az) dz. \quad (\text{A18})$$

The position $z_1(p, t)$ is defined by the solution of

$$b_0 B_H^2 \zeta(z_1) p t = 1. \quad (\text{A19})$$

For $z < z_1$ we have $a = (4Dt)^{-1/2}$, and for $z > z_1$ we have $a = (b_0 B_H^2 p / 4D)^{1/2}$, in equation (A18).

The simplest case is that of early times, or low energies. For $b_0 B_H^2 p t < 1$, there is no solution to equation (A19), so that the ‘‘early’’ expression for a applies everywhere. The solution in equation (A18) then gives

$$N(p, t) = \frac{\phi_0}{p^2} \left(\frac{4Dt}{\pi} \right)^{1/2}. \quad (\text{A20})$$

This has the same power-law form as the reservoir, and its magnitude increases in proportion to $t^{1/2}$.

For higher energies, or later times, the integral in equation (A18) may be broken at z_1 :

$$N(p, t) = \frac{\phi_0}{p^2} \left[\int_0^{z_1} \text{erfc} \left(\frac{z}{\sqrt{4Dt}} \right) dz + \int_{z_1}^\infty \text{erfc} \left(z \sqrt{\frac{q}{4D}} \right) dz \right]. \quad (\text{A21})$$

The formal solution to equation (A21) is

$$N(p, t) = \frac{\phi_0}{p^2} z_1 \left\{ \text{erfc} \left(\frac{z_1}{\sqrt{4Dt}} \right) - \text{erfc} \left(z_1 \sqrt{\frac{q}{4D}} \right) + \sqrt{\frac{4Dt}{z_1^2 \pi}} \left[1 - \exp \left(\frac{-z_1^2}{4Dt} \right) \right] + \sqrt{\frac{4D}{z_1^2 \pi q}} \exp \left(\frac{-z_1^2 q}{4D} \right) \right\}, \quad (\text{A22})$$

where we write $q = b_0 B_H^2 p$ to shorten the notation. Expanding the complementary error function and the exponential in the limit of large and small argument, for $L \gg (4Dt)^{1/2}$ we find two significant energy cutoffs, which define three ranges, for the functional form of $N(p, t)$. The two critical energies are

$$p_{c1} = \frac{1}{b_0 B_H^2 t} \frac{L}{\sqrt{4Dt}}, \quad p_{c2} = \frac{1}{b_0 B_H^2 t} \frac{L^2}{4Dt}. \quad (\text{A23})$$

At low energies, $p < p_{c1}$, the integrated solution is

$$N(p, t) \simeq \frac{\phi_0}{p^2} \left(\frac{4Dt}{\pi} \right)^{1/2}, \quad (\text{A24})$$

which recovers the reservoir power law again. At intermediate energies, $p_{c1} < p < p_{c2}$, the solution is

$$N(p, t) \simeq \frac{\phi_0}{p^2} \frac{L}{b_0 B_H^2 p t} \left(1 - \frac{1}{\sqrt{\pi}} \frac{L}{b_0 B_H^2 p t \sqrt{4Dt}} \right), \quad (\text{A25})$$

and at high energies, $p > p_{c2}$, the integrated DF steepens:

$$N(p, t) \simeq \frac{\phi_0}{p^2} \left(\frac{4D}{\pi b_0 B_H^2 p} \right)^{1/2}. \quad (\text{A26})$$

Thus, the high-energy solution is a slightly steeper power law than the reservoir. There is an increase from the low-energy form ($b = 4$) to the high-energy form ($b = 4.5$) with the intermediate-energy solution providing a smooth join between them.

We can also integrate the synchrotron emissivity:

$$J_{\text{sy}}(\nu, t) = \int_0^\infty j_{\text{sy}}(z, \nu, t) dz = \frac{J_0}{\nu^{1/2}} \int_0^\infty [\zeta(z)]^{3/4} \operatorname{erfc}(az) dz, \quad (\text{A27})$$

where a is interpreted as in equation (A14). The break position, $z_1(\nu, t)$, is now given by

$$A^2 \nu \zeta^{3/2}(z_1) t^2 = 1, \quad (\text{A28})$$

which gives $z_1(\nu, t) \simeq L(A\nu^{1/2}t)^{-4/3}$. We must pick a specific ramp function in order to evaluate equation (A27). We take $\zeta(z) = (1 - e^{-z/L})^{4/3}$, which specifies the spatial scale L , while allowing equation (A27) to be evaluated analytically. For low frequencies, $\nu < 1/A^2 t^2$, we find

$$J_{\text{sy}}(\nu, t) = \frac{J_0 L}{\nu^{1/2}} \left[-1 + \exp\left(\frac{1}{4a_y^2 L^2}\right) \frac{2}{\sqrt{\pi}} \Gamma\left(\frac{3}{2}, \frac{1}{4a_y^2 L^2}\right) \right], \quad (\text{A29})$$

where $\Gamma(3/2, x)$ is the incomplete gamma function. In the interesting limit, $L \gg (4Dt)^{1/2}$, this simplifies to

$$J_{\text{sy}}(\nu, t) \simeq J_0 \nu^{-1/2} \frac{Dt}{L}. \quad (\text{A30})$$

For higher frequencies, we again break the integral:

$$J_{\text{sy}}(\nu, t) = \frac{J_0}{\nu^{1/2}} \left[\int_0^{z_1} \zeta(z) \operatorname{erfc}\left(\frac{z}{\sqrt{4Dt}}\right) dz + \int_{z_1}^\infty \zeta(z) \operatorname{erfc}\left(z\sqrt{\frac{q}{4D}}\right) dz \right]. \quad (\text{A31})$$

The formal solution of this is

$$\begin{aligned} J_{\text{sy}}(\nu, t) = \frac{J_0}{\nu^{1/2}} \left\{ -L + \frac{1}{a_y \sqrt{\pi}} [1 - \exp(-a_y^2 z_1^2)] + (Le^{-z_1/L} + z_1) \operatorname{erfc}(a_y z_1) \right. \\ + L \exp\left(\frac{1}{4a_y^2 L^2}\right) \left[\operatorname{erfc}\left(\frac{1}{2a_y L}\right) - \operatorname{erfc}\left(a_y z_1 + \frac{1}{2a_y L}\right) \right] \\ - (Le^{-z_1/L} + z_1) \operatorname{erfc}(a_0 z_1) - \frac{1}{a_0 \sqrt{\pi}} [1 - \exp(-a_0^2 z_1^2)] \\ \left. + L \exp\left(\frac{1}{4a_0^2 L^2}\right) \left[\frac{2}{\sqrt{\pi}} \Gamma\left(\frac{3}{2}, \frac{1}{4a_0^2 L^2}\right) - \operatorname{erfc}\left(\frac{1}{2a_0 L}\right) + \operatorname{erfc}\left(a_0 z_1 + \frac{1}{2a_0 L}\right) \right] \right\}. \quad (\text{A32}) \end{aligned}$$

As with the integrated DF, we find two critical frequencies, at which the spectrum changes shape:

$$\nu_{c1} = \frac{1}{(At)^2} \left(\frac{L}{\sqrt{4Dt}}\right)^{3/2}, \quad \nu_{c2} = \frac{1}{(At)^2} \left(\frac{L}{\sqrt{4Dt}}\right)^{12/5}. \quad (\text{A33})$$

There are three frequency ranges. For low frequencies, $\nu < \nu_{c1}$,

$$J_{\text{sy}}(\nu, t) \simeq J_0 \frac{Dt}{L} \nu^{-1/2}. \quad (\text{A34})$$

For intermediate frequencies, $\nu_{c1} < \nu < \nu_{c2}$,

$$J_{\text{sy}}(\nu, t) \simeq J_0 \frac{Dt}{L} \left(1 + \frac{1}{A\nu^{1/2}t}\right) \nu^{-1/2}. \quad (\text{A35})$$

Finally, for high frequencies, $\nu > \nu_{c2}$,

$$J_{\text{sy}}(\nu, t) \simeq \frac{J_0 D}{AL} \nu^{-1}. \quad (\text{A36})$$

APPENDIX B

THE LEAKY BOX MODEL

It is convenient to write equations (3.1) and (3.2) in matrix form:

$$[f] = \begin{pmatrix} f_1 \\ f_2 \end{pmatrix}, \quad [Q] = \begin{pmatrix} Q_1 \\ Q_2 \end{pmatrix}, \quad [r] = \begin{pmatrix} r_{11} & -r_{12} \\ -r_{21} & r_{22} \end{pmatrix}, \quad [B^2] = \begin{pmatrix} B_1^2 & 0 \\ 0 & B_2^2 \end{pmatrix}. \quad (\text{B1})$$

Then equations (3.1) and (3.2) become

$$\frac{\partial [f(p)]}{\partial t} = \frac{b_0}{p_2} [B^2] \frac{\partial}{\partial p} \{p^4 [f(p)]\} - [r][f(p)] + [Q(p)]. \quad (\text{B2})$$

Denoting Laplace-transformed quantities by a tilde, equation (B2) gives

$$s[\tilde{f}(p, s)] - [f(p)]_0 = \frac{b_0}{p^2} [B^2] \frac{\partial}{\partial p} \{p^4 [\tilde{f}(p, s)]\} - [f][\tilde{f}(p, s)] + [\tilde{Q}(p, s)]. \quad (\text{B3})$$

The integrating factor is a matrix:

$$[M(p, s)] = \exp \left\{ \frac{1}{b_0 p} [B^2]^{-1} (s[1] + [r]) \right\}, \quad (\text{B4})$$

and the solution of equation (B3) is

$$[\tilde{f}(p, s)] = \frac{1}{b_0 p^4} \int_p d p' p'^2 [H(p, p', s)] [B^2]^{-1} \{ [f(p')]_0 + [\tilde{Q}(p', s)] \}, \quad (\text{B5})$$

where s now appears only in the *transfer matrix*

$$[H(p, p', s)] = [M(p, s)]^{-1} [M(p', s)]. \quad (\text{B6})$$

Explicit evaluation of the transfer matrix gives

$$H(p, p', s) = \exp \left\{ [B^2]^{-1} ([r] + s[1]) \frac{1}{b_0} \left(\frac{1}{p'} - \frac{1}{p} \right) \right\}. \quad (\text{B7})$$

We are unable to invert the Laplace transform to solve equation (B5) to find $f_1(p, t)$, $f_2(p, t)$ explicitly.

The asymptotic solution follows from the limits $s \rightarrow 0$. Assuming that the number of particles is conserved, that is $r_{11} r_{22} = r_{12} r_{21}$, in the limit $s = 0$, equation (B7) gives

$$H(p, p', 0) = [1] + \frac{2e^\rho \sinh \rho}{B_L^{-2} r_{11} + B_H^{-2} r_{22}} [B^2]^{-1} [r], \quad (\text{B8})$$

with

$$\rho = p_0 \left(\frac{1}{p'} - \frac{1}{p} \right), \quad p_0 = \frac{1}{2b_0} (B_L^{-2} r_{11} + B_H^{-2} r_{22}). \quad (\text{B9})$$

The asymptotic solution follows from equation (B5):

$$[f(p, \infty)] = \frac{1}{b_0 p^4} \int_p d p' p'^2 [H(p, p', 0)] [B^2]^{-1} \{ [f(p')]_0 + [\tilde{Q}(p', s)] \}. \quad (\text{B10})$$

Assuming $f_1(p, 0) = f_2(p, 0) = 0$, $Q_2(p, t) = 0$, and $Q_1(p)$ independent of t , equation (B10) gives equations (3.8) and (3.9).

REFERENCES

- Alexander, P., & Leahy, J. P. 1987, MNRAS, 225, 1
 Baldwin, J. E. 1982, in IAU Symp. 97, Extragalactic Radio Sources, ed. D. S. Heeschen & C. M. Wade (Dordrecht: Reidel), 21
 Berezhinskii, V. S., Bulanov, S. V., Dogiel, V. A., Ginzburg, V. L., & Ptuskin, V. S. 1990, Astrophysics of Cosmic Rays (Amsterdam: North-Holland)
 Carilli, C. L., Perley, R. A., Dreher, J. W., & Leahy, J. P. 1991, ApJ, 383, 554
 Comins, N. F., & Owen, F. N. 1991, ApJ, 382, 108
 Eilek, J. A. 1993, in Jets in Extragalactic Radio Sources, ed. J.-H. Röser & K. Meisenheimer (New York: Springer), 279
 ———. 1996, in Energy Transport in Radio Galaxies and Quasars, ed. P. E. Hardee, A. H. Bridle, & J. A. Zensus (San Francisco: ASP), in press
 ———. 1997, ApJ, submitted
 Eilek, J. A., & Arendt, P. N. 1996, ApJ, 457, 150
 Felten, J. E. 1968, ApJ, 151, 861
 Fomalont, E. B., Ebneter, K. A., van Breugel, W. J. M., & Ekers, R. D. 1989, ApJ, 346, L17
 Ginzburg, V. L., & Syrovatskii, S. I. 1964, The Origin of Cosmic Rays (New York: Macmillan)
 Hines, D. C., Owen, F. N., & Eilek, J. A. 1989, ApJ, 347, 713
 Hughes, P. E. 1979, MNRAS, 186, 853
 Jokipii, J. R., & Parker, E. N. 1966, ApJ, 155, 777
 Kardashev, N. S. 1962, Soviet Astron.—AJ, 6, 317
 Katz-Stone, D. M., Rudnick, L., & Andersen, M. C. 1993, ApJ, 407, 549
 Meisenheimer, K., Röser, H.-J., & Schlötelburg, M. 1996, A&A, 307, 61
 Melrose, D. B. 1970, Ap&SS, 6, 321
 O'Donoghue, A. A., Eilek, J. A., & Owen, F. N. 1993, ApJ, 408, 428
 O'Donoghue, A. A., Owen, F. N., & Eilek, J. A. 1990, ApJS, 72, 75
 Owen, F. N. 1993, in Jets in Extragalactic Radio Sources, ed. H.-J. Röser & K. Meisenheimer (New York: Springer), 273
 Owen, F. N., Hardee, P. E., & Cornwell, T. J. 1989, ApJ, 340, 698
 Owen, F. N., O'Dea, C. P., Inoue, M., & Eilek, J. A. 1985, ApJ, 294, L85
 Pacholczyk, A. G. 1970, Radio Astrophysics (San Francisco: Freeman)
 Perley, R. A., Dreher, J. W., & Cowan, J. J. 1984, ApJ, 285, L35
 Pouquet, A., Frisch, U., & Leorat, J. 1976, J. Fluid Mech., 77, 321
 Spangler, S. R. 1979, ApJ, 232, L7
 Walker, M., Melrose, D., & Ball, L. 1994, in The Physics of Active Galaxies, ed. G. Bicknell, M. Dopita, & P. Quinn (San Francisco: ASP), 377
 Willis, A. G., & Strom, R. G. 1978, A&A, 62, 375
 Zwaan, C. 1987, Ann. Rev. A&A, 25, 83